



Ironless Permanent Magnet Motors: Three-Dimensional Analytical Calculation

Romain Ravaud, Guy Lemarquand, Valérie Lemarquand

► To cite this version:

Romain Ravaud, Guy Lemarquand, Valérie Lemarquand. Ironless Permanent Magnet Motors: Three-Dimensional Analytical Calculation. IEEE International Electric Machines and Drives Conference IEMDC'09, May 2009, Miami, United States. pp.947-952, 10.1109/IEMDC.2009.5075318 . hal-00413352

HAL Id: hal-00413352

<https://hal.science/hal-00413352>

Submitted on 3 Sep 2009

HAL is a multi-disciplinary open access archive for the deposit and dissemination of scientific research documents, whether they are published or not. The documents may come from teaching and research institutions in France or abroad, or from public or private research centers.

L'archive ouverte pluridisciplinaire **HAL**, est destinée au dépôt et à la diffusion de documents scientifiques de niveau recherche, publiés ou non, émanant des établissements d'enseignement et de recherche français ou étrangers, des laboratoires publics ou privés.

Ironless Permanent Magnet Motors: Three-Dimensional Analytical Calculation

Romain Ravaut, Guy Lemarquand, *Senior Member, IEEE*, Valerie Lemarquand

Abstract—We present a three-dimensional expression of the magnetic torque exerted between a tile permanent magnet radially magnetized and a winding in ironless structures. Such an expression can be used for calculating the magnetic torque transmitted between the stator and the rotor of an ironless permanent magnet motor. The calculations are carried out without using any simplifying assumptions. Consequently, the expression of the torque obtained is exact whatever the magnet or winding dimensions. The ironless structure we consider in this paper is commonly used for high speed rotation devices in which eddy currents must be avoided. Indeed, it is noted that more and more structures are ironless because they offer promising perspectives.

Index Terms—Ironless motor, analytical calculations, torque, magnetic field, PM Synchronous motors

1 INTRODUCTION

IRONLESS electrical machines are generally used when high-speed rotations are required. These ironless motors [1][4] differ from iron-core motors [5][6] because the last ones are used up to a few hundred of hertz. Even though ironless motors are less efficient than iron-core motors, they constitute technological solutions [7][8] for avoiding the drawbacks of eddy currents that appear in iron-core motors. Many studies on ironless structures have been performed by several authors [9][10] with analytical or semi-analytical approaches. In addition, some studies dealing with iron-core electric machines have been carried out with different analytical calculations [11][12]. Strictly speaking, iron-core motors using permanent magnets and windings are composed of iron parts whose aim is to confine the magnetic field produced by the permanent magnets. However, for high speed rotation devices, the presence of iron is problematic in the structure because eddy currents appear. Nevertheless, it is well known that the presence of these eddy currents generates a decrease in the efficiency

of the torque transmitted between the stator and the rotor of electrical machines. This is why we can say that two kinds of applications must be identified and depend on both the input frequency and the rotation speed required. In addition, the magnet topology is also of great importance in high-speed motors and must be clearly optimized [13].

Several methods can be used for studying analytically ironless motors [14]–[19]. These methods generally use the three-dimensional magnetic potential created by permanent magnets [21] and allow us to optimize easily such structures [22]–[24].

Consequently, high speed rotation devices are only composed of ironless parts with samarium-cobalt magnets that are not conductor of electricity. The efficiency of such ironless structures is weaker than iron electrical machines but they can reach very high rotating speeds without the drawbacks of the eddy current effects. The accurate knowledge of the torque in such ironless structures is required for optimization purposes. It is noted that a semi-analytical calculation of this torque is possible because the structure considered is ironless. For classical electrical machines, such calculations are more difficult and finite-element methods are appropriate.

• The authors are with the Laboratoire d'Acoustique de l'Université du Maine, LAUM, UMR CNRS 6613, Le Mans, 72025 Cedex
E-mail: guy.lemarquand@ieee.org

We present in this paper an analytical calculation of the torque transmitted between the stator and the rotor of an ironless motor. We use the analogy between the coulombian model and the amperian current model for calculating the torque transmitted between a tile permanent magnet radially magnetized and a winding in the stator. Then, by using the principle of superposition, this calculation is used for calculating the torque transmitted between the stator and the rotor.

2 NOTATION AND GEOMETRY

The geometry considered and the related parameters are shown in Fig 1. We consider both an outer tile permanent magnet and an inner winding. Such a configuration corresponds to an element of an ironless permanent magnet motor. Both the tile permanent magnet and the winding can be modeled by using the coulombian model. Indeed, by using the analogy between the coulombian and the amperian current models, the winding can be represented by using the fictive magnetic pole densities that are located on both the inner and outer surfaces delimited by the winding. The radially magnetized tile permanent magnet is also represented by fictitious magnetic pole surface densities [8] that are located on its inner and outer faces as well as in its volume. We denote H_θ , the azimuthal component of the magnetic field created by the tile permanent magnet. Its expression is given by

$$H_\theta = \vec{H}(r, \theta, z) \cdot \vec{u}_\theta \quad (1)$$

where

$$\vec{H}(r, \theta, z) = -\vec{\nabla}(\Phi(r, \theta, z)) \quad (2)$$

and $\Phi(r, \theta, z)$ is the scalar magnetic potential produced by the tile permanent magnet radially magnetized. This scalar magnetic potential

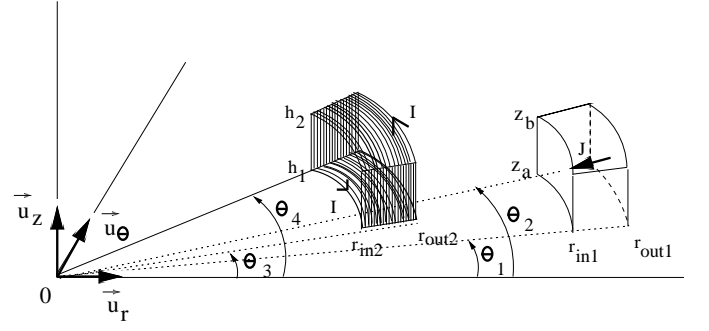


Fig. 1. Geometry considered: an outer tile permanent magnet radially magnetized (polarization J) and an inner winding with a current, I , flowing through it. The inner radius of the outer tile permanent magnet is r_{in1} and its outer radius is r_{out1} . Its height is $z_b - z_a$ and its angular width is $\theta_2 - \theta_1$. Its magnetic polarization is denoted J . The inner radius of the winding is r_{in2} and its outer radius is r_{out2} . Its height is $h_2 - h_1$ and its angular width is $\theta_4 - \theta_3$.

is expressed as follows:

$$\begin{aligned} \Phi(r, \theta, z) = & \frac{1}{4\pi} \int \int_{S'_{in}} \frac{J}{|\vec{r} - \vec{r}'|} r_{in1} d\theta_1 dz_1 \\ & - \frac{1}{4\pi} \int \int_{S'_{out}} \frac{J}{|\vec{r} - \vec{r}'|} r_{out1} d\theta_1 dz_1 \\ & + \frac{1}{4\pi} \int \int \int_{V'} \frac{J}{|\vec{r} - \vec{r}'|} dr_1 d\theta_1 dz_1 \end{aligned} \quad (3)$$

where $|\vec{r} - \vec{r}'|$ is the distance between the observation point and a point located on the charge distribution, S'_{in} is the inner surface of the tile permanent magnet, S'_{out} is the outer surface of the tile permanent magnet and V' is its volume. In addition, K , the equivalent charge densities of the winding, is defined as follows:

$$K = \frac{\mu_0 N I}{(r_{out2} - r_{in2})} \quad (4)$$

where μ_0 is the permeability of the vacuum, I is the intensity flowing in the winding and N is the number of current loops. In the numerical simulation carried out in this paper, we have taken $NI = 240$ At and $K=0.1$ T.

The magnetic torque can be determined as

Parameters	Expressions
$T_1(a, b)$	$-a^2b^2JK(g(\theta_2) - g(\theta_1))/4\pi\mu_0$
$T_2(a, b)$	$-ab^2JK(g(\theta_2) - g(\theta_1))/4\pi\mu_0$
$T_3(a, b)$	$-a^2bJK(g(\theta_2) - g(\theta_1))/4\pi\mu_0$
$T_4(a, b)$	$-abJK(g(\theta_2) - g(\theta_1))/4\pi\mu_0$

TABLE 1

Parameters used for calculating the torque transmitted between a permanent magnet and a winding

follows:

$$\begin{aligned}
T = & \int \int_{S_{in2}} H_\theta K r_{in2} d\tilde{S}_{in2} \\
& - \int \int_{S_{out2}} H_\theta K r_{out2} d\tilde{S}_{out2} \\
& + \int \int \int_V H_\theta K d\tilde{V}
\end{aligned} \quad (5)$$

where V is the volume of the winding, S_{in2} and S_{out2} are its inner and outer faces. The azimuthal component H_θ of the magnetic field created by the outer tile permanent magnet can be determined either by using the scalar magnetic potential, the vector potential or the three-dimensional Green's function [7]. Without any simplifying assumptions, there are up to six integrations necessary for calculating the magnetic torque. However, this expression can also be reduced to the following form:

$$\begin{aligned}
T = & \int_{\theta_3}^{\theta_4} (T_1(r_{out1}, r_{out2}) - T_1(r_{in1}, r_{out2})) d\theta_i \\
& + \int_{\theta_3}^{\theta_4} (T_1(r_{in1}, r_{in2}) - T_1(r_{out1}, r_{in2})) d\theta_i \\
& + \int_{\theta_3}^{\theta_4} \int_{r_{in1}}^{r_{out1}} (T_2(r_1, r_{in2})) dr_1 d\theta_i \\
& - \int_{\theta_3}^{\theta_4} \int_{r_{in1}}^{r_{out1}} (T_2(r_1, r_{out2})) dr_1 d\theta_i \\
& + \int_{\theta_3}^{\theta_4} \int_{r_{in2}}^{r_{out2}} (T_3(r_2, r_{in1})) dr_2 d\theta_i \\
& - \int_{\theta_3}^{\theta_4} \int_{r_{in2}}^{r_{out2}} (T_3(r_2, r_{out1})) dr_2 d\theta_i \\
& + \int_{\theta_3}^{\theta_4} \int_{r_{in1}}^{r_{out1}} \int_{r_{in2}}^{r_{out2}} T_4(r_1, r_2) d\theta_i dr_1 dr_2
\end{aligned} \quad (6)$$

The parameters used in (6) are defined in Table 1. Furthermore, the functions used in Table 1

are defined as follows:

$$\begin{aligned}
g(\theta_j) = & y(a, b, h_2, z_a) - y(a, b, h_1, z_a) \\
& + y(a, b, h_1, z_b) - y(a, b, h_2, z_b)
\end{aligned} \quad (7)$$

with

$$y(a, b, z_1, z_2) = -\frac{\eta}{ab} \arctan \left[\frac{\xi}{\eta} \right] + \frac{\xi}{ab} \quad (8)$$

and

$$\begin{aligned}
\xi = & \sqrt{a^2 + b^2 + (z_2 - z_1)^2 - 2ab \cos(\theta_i - \theta_j)} \\
\eta = & \sqrt{-(z_1 - z_2)^2}
\end{aligned} \quad (10)$$

The expression obtained can be used for realizing easily parametric studies. It is emphasized here that Eq. (2) contains three types of interactions that correspond to the interactions between the surface and volume densities of the tile and of the winding. In addition, the numerical integrations of Eq. (4) have a robust convergence. As a consequence, the determination of Eq. (2) is both fast and accurate and allows us to study the magnetic torque transmitted by several radially magnetized tile permanent magnets on several windings.

3 APPLICATION: MAGNETIC TORQUE IN AN IRONLESS PERMANENT MAGNET MOTOR

We discuss now the interest of using such an analytical expression for calculating the magnetic torque transmitted in an ironless permanent magnet motor. For this purpose, let us consider a motor whose rotor bears n radially magnetized permanent magnets and whose stator bears k windings. The total magnetic torque can be expressed as follows:

$$T_{total} = \sum_{i=1}^n \sum_{j=1}^k \alpha^{(i,j)} T_{i,j} \quad (11)$$

where i represents the i^{th} magnet of the rotor, j represents the j^{th} winding of the stator and $T_{i,j}$ represents the magnetic torque transmitted between the i^{th} magnet and the j^{th} winding. The parameter $\alpha^{(i,j)}$ is 1 if the magnet and winding polarizations are in the same sense and -1 if

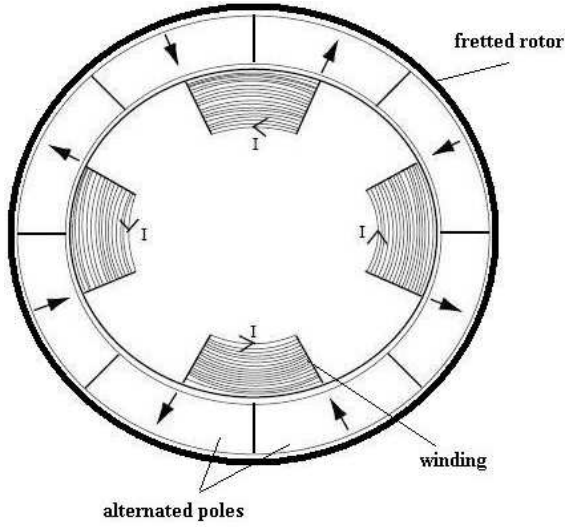


Fig. 2. Ironless permanent magnet motor with 8 radially magnetized permanent magnets in its outer rotor and 4 windings in its inner stator.

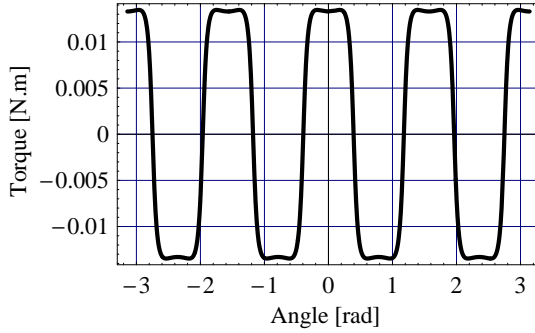


Fig. 3. Representation of the torque T versus the angular shift between the stator and the rotor, $r_{in1} = 0.025$ m, $r_{out1} = 0.028$ m, $r_{in2} = 0.021$ m, $r_{out2} = 0.024$ m, $J=1$ T, $K=0.1$ T for the three representations and all the tiles have the same height $h=0.003$ m.

their polarizations are opposite. We illustrate it with the following set of parameters: $n = 8$, $k = 4$, as shown in Fig. 2. The total magnetic torque transmitted by the stator on the rotor is represented versus the angular shift in Fig. 2 in which we give the numerical results given by the three-dimensional expression of the torque transmitted between a rotor with 8 radially magnetized tile permanent magnets and a stator with 4 windings. In addition, it is to be noted that no simplifying assumption is done and that the computational cost is nevertheless very low (less than 250s). This computational

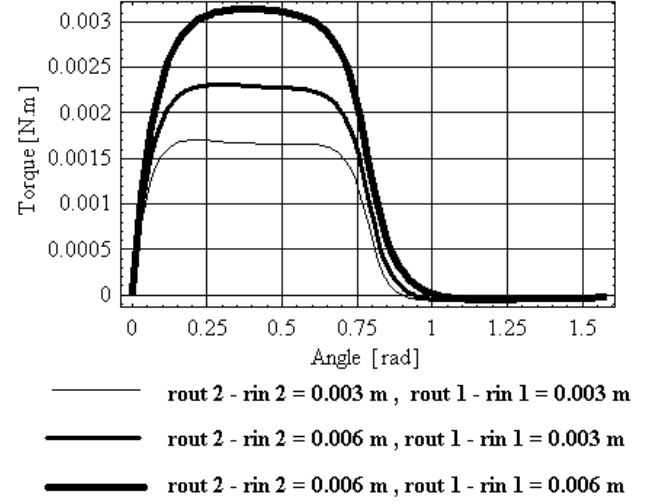


Fig. 4. Representation of the torque T versus the angular shift between one permanent magnet and a winding, $J= 1$ T, $K=0.1$ T and all the tiles have the same height $h= 0.003$ m.

cost can still be dropped by neglecting the term owing three numerical integrals in Eq. (2). Such simplifications can safely be done because the interactions between the fictitious volume charges have not a great influence on the torque calculation between the winding and the tile permanent magnet.

4 INFLUENCE OF THE POLE RADIAL WIDTHS ON THE TORQUE TRANSMITTED BETWEEN THE STATOR AND THE ROTOR

In our configuration, the number of poles and the permanent magnet and winding dimensions have a great influence on the torque transmitted between the stator and the rotor. By using the analytical calculations established in this paper, it is possible to optimize the permanent magnet dimensions in order to obtain the greatest torque. We illustrate in Fig. 4 how varies the torque transmitted between one permanent magnet at the rotor and one winding in the stator when their radial widths increase by keeping the same equivalent charge density $K = 0.1$ T. Figure 4 shows that the more the radial widths are important, the more the torque transmitted between the permanent magnet and the winding is. However, other parameters must be taken into account as the

magnet volume [25] and the structure dimensions [26]. Such optimizations are possible with analytical calculations as they are fast to carry out.

5 CONCLUSION

This paper presents an exact three-dimensional analytical method for calculating the torque transmitted between the stator and the rotor of ironless permanent magnet motors with radially magnetized tile permanent magnets and windings. Such structures are generally used when high-speed rotations are required. It is emphasized that the calculations have been carried out without using any simplifying assumptions. The expression of the torque is obtained in a semi-analytical form that can be still simplified by neglecting the interactions between the charge volume densities. Indeed, this interaction has a very low influence of the torque value. In addition, the computational cost of such an expression being very low, this approach is a good alternative to the finite-element methods for carrying out parametric studies in ironless structures. However, it must be emphasized that such calculations can be carry out analytically possible because the structure considered is ironless.

REFERENCES

- [1] N. Boules, "Prediction of no-load flux density distribution in permanent magnet machines," *IEEE Trans. Ind. Appl.*, vol. IA-21, no. 3, pp. 633–643, 1985.
- [2] F. Caricchi, F. Crescimbeni, O. Honorati, G. L. Bianco, and E. Santini, "Performance of coreless-winding axial-flux permanent-magnet generator with output at 400Hz,3000tr/min," *IEEE Trans. Ind. Appl.*, vol. 34, no. 6, pp. 1263–1269, 1998.
- [3] N. F. Lombard and M. J. Kamper, "Analysis and performance of an ironless stator axial flux pm machine," *IEEE Trans. Energy Conversion*, vol. 14, no. 4, pp. 1051–1056, 1999.
- [4] J. de Boeij, E. Lomonova, and A. Vandenput, "Modeling ironless permanent-magnet planar actuator structures," *IEEE Trans. Magn.*, vol. 42, no. 8, pp. 2009–2016, 2006.
- [5] E. Muljadi, C. P. Butterfield, and Y.-H. Wan, "Axial-flux modular permanent-magnet generator with a toroidal winding for wind-turbine applications," *IEEE Trans. Ind. Appl.*, vol. 35, no. 4, pp. 831–836, 1999.
- [6] M. J. Kamper, R.-J. Wang, and F. G. Rossouw, "Analysis and performance of axial flux permanent-magnet machine with air-cored nonoverlapping concentrated stator windings," *IEEE Trans. Ind. Appl.*, vol. 44, no. 5, pp. 1495–1504, 2008.
- [7] W. Baran and M. Knorr, "Synchronous couplings with sm co5 magnets," pp. 140–151, 2nd Int. Workshop on Rare-Earth Cobalt Permanent Magnets and Their Applications, Dayton, Ohio, USA, 1976.
- [8] S.-M. Jang, D.-J. You, K.-J. Ko, and S.-K. Choi, "Design and experimental evaluation of synchronous machine without iron loss using double-sided halbach magnetized pm rotor in high power fess," *IEEE Trans. Magn.*, vol. 44, no. 5, pp. 4337–4340, 2008.
- [9] U. K. Madawala and J. T. Boys, "Magnetic field analysis of an ironless brushless dc machine," *IEEE Trans. Magn.*, vol. 41, no. 8, pp. 2384–2390, 2005.
- [10] P. Ragot, M. Markovic, and Y. Perriard, "Optimization of electric motor for a solar airplane application," *IEEE Trans. Ind. Appl.*, vol. 42, no. 4, pp. 1053–1061, 2006.
- [11] Z. Zhu, Z. Xia, and D. Howe, "Comparison of halbach magnetized brushless machines based on discrete magnet segments or a single ring magnet," *IEEE Trans. Magn.*, vol. 38, no. 9, pp. 2997–2999, 2002.
- [12] Z. Zhu and D. Howe, "Analytical prediction of the cogging torque in radial-field permanent magnet brushless motors," *IEEE Trans. Magn.*, vol. 28, no. 2, pp. 1371–1374, 1992.
- [13] T. S. El-Hasan and P. C. K. Luk, "Magnet topology optimization to reduce harmonics in high-speed axial flux generators," *IEEE Trans. Magn.*, vol. 39, no. 5, pp. 3340–3342, 2003.
- [14] S. Babic and C. Akyel, "An improvement in the calculation of the magnetic field for an arbitrary geometry coil with rectangular cross section," *International Journal of Numerical Modelling: Electronic Networks, Devices and Fields*, vol. 18, pp. 493–504, November 2005.
- [15] S. Babic and C. Akyel, "Improvement in the analytical calculation of the magnetic field produced by permanent magnet rings," *Progress in Electromagnetics Research C*, vol. 5, pp. 71–82, 2008.
- [16] B. Azzerboni and G. Saraceno, "Three-dimensional calculation of the magnetic field created by current-carrying massive disks," *IEEE Trans. Magn.*, vol. 34, no. 5, pp. 2601–2604, 1998.
- [17] J. P. Selvaggi, S. Salon, O. M. Kwon, and M. V. K. Chari, "Computation of the three-dimensional magnetic field from solid permanent-magnet bipolar cylinders by employing toroidal harmonics," *IEEE Trans. Magn.*, vol. 43, no. 10, pp. 3833–3839, 2007.
- [18] E. P. Furlani, *Permanent Magnet and Electromechanical Devices: Materials, Analysis and Applications*. Academic Press, 2001.
- [19] R. Ravaud, G. Lemarquand, V. Lemarquand, and C. Depollier, "Discussion about the analytical calculation of the magnetic field created by permanent magnets," *Progress in Electromagnetics Research B*, vol. 11, pp. 281–297, 2009.
- [20] R. Ravaud and G. Lemarquand, "Modelling an ironless loudspeaker by using three-dimensional analytical approaches," *Progress in Electromagnetics Research, PIER 91*, pp. 53–68, 2009.
- [21] R. Ravaud, G. Lemarquand, V. Lemarquand, and C. Depollier, "Torque in permanent magnet couplings: comparison of uniform and radial magnetization," *Journal of applied physics*, vol. 105, no. 5, 2009.
- [22] G. Lemarquand, "Ironless loudspeakers," *IEEE Trans. Magn.*, vol. 43, no. 8, pp. 3371–3374, 2007.
- [23] R. Ravaud, G. Lemarquand, V. Lemarquand, and C. Depollier, "Analytical calculation of the magnetic field cre-

- ated by permanent-magnet rings," *IEEE Trans. Magn.*, vol. 44, no. 8, pp. 1982–1989, 2008.
- [24] R. Ravaut, G. Lemarquand, V. Lemarquand, and C. Depollier, "The three exact components of the magnetic field created by a radially magnetized tile permanent magnet," *Progress in Electromagnetics Research, PIER 88*, pp. 307–319, 2008.
 - [25] J. F. Charpentier and G. Lemarquand, "Calculation of ironless permanent magnet coupling using semi-numerical magnetic pole theory method," *COMPEL*, vol. 20, no. 1, pp. 72–89, 2001.
 - [26] V. Lemarquand, J. F. Charpentier, and G. Lemarquand, "Nonsinusoidal torque of permanent-magnet couplings," *IEEE Trans. Magn.*, vol. 35, no. 5, pp. 4200–4205, 1999.